

# Near well simulation of extra-heavy oil production using SAGD

<sup>1</sup>Kou Guandong <sup>1</sup>Britt Halvorsen

<sup>1</sup>Department of Technology, Telemark University College, Norway

## Abstract

Steam-Assisted Gravity Drainage (SAGD) is an enhanced oil recovery method. One challenge for SAGD process is that part of the injected steam flows directly into the production well without condensation, which causes energy loss and lower oil production rate. Autonomous Inflow Control Valves (AICVs) can shut off water and gas autonomously, and can therefore be useful in the SAGD process. The multiphase simulator OLGA in combination with the near well simulation tool ROCX are used for simulation of the application of AICVs in the SAGD process.

The result shows that AICVs are able to close for water (and thereby also for steam), and the closing time depends on controller set point of water cut. It is also observed that the production rate of water increases significantly after water breakthrough.

**Keywords:** SAGD, AICV, simulation, heavy oil, bitumen, reservoir, OLGA, ROCX, flow rate, permeability

## 1 Introduction

Nowadays, demand for heavy oil and bitumen is increasing, since conventional oil has limited amount and oscillating price. Thermal methods are often used for producing heavy oil, among them the Steam-Assisted Gravity Drainage (SAGD) process is one of the most widely used. The basic mechanism in SAGD is that heavy oil is heated up by injected steam from the injection well, and as a result the heavy oil becomes less viscous and mobile and can be produced from the production well. (Speight, 2013) Autonomous Inflow Control Valves (AICVs) can also be used in the SAGD process for production of heavy oil and bitumen, since it can shut off water and increase the oil recovery rate.

In this study, the theoretical background of heavy oil and common production methods are first introduced. Besides, a program for calculating required steam injection amount is developed in MATLAB. (mathworks, 2015) In addition, fundamental knowledge of AICV and the simulation software OLGA (Schlumberger) are briefly demonstrated. Moreover, the simulation of the SAGD process combined with AICVs are performed, with the result presented and discussed. Finally, limitations and prospects of this study are provided.

## 1.1 Heavy oil and bitumen

Heavy oil is characterized as an asphaltic, dense, viscous nature, and its asphaltene content, as defined by the U.S. Geological Survey (Meyer, 2003).

Although variously defined, the upper limit for heavy oil is 22° API gravity with a viscosity of 100 centipoise (cP) (Meyer, 2003). API gravity is short for "American Petroleum Institute's gravity", and is used as a standard to express the specific weight of oil. The equation for calculating the API gravity is shown in equation (1).

$$\text{API gravity} = \frac{141.5}{SG} - 131.5 \quad (1)$$

where SG stands for specific gravity of oil.

Based on this criterion, light oil and extra heavy oil are also explained respectively in the following. Oil with at least 22° API gravity and a viscosity less than 100 cP is known as conventional oil (Meyer, 2003). Extra heavy oil is the portion of heavy oil having an API gravity of less than 10°. In comparison with light oil, heavy or extra heavy oil cannot flow naturally and has to be heated or diluted to be pumped out.

Bitumen shares the attributes of heavy oil but is even more dense and viscous. Natural bitumen has a viscosity higher than 10,000 cP. Extra-heavy oil natural bitumen is also known as "oil sands". (Banerjee, 2012)

In Canada, bitumen is regarded as the crude obtained from oil sands. However, it should be noted that oil sands are often incorrectly called tar sands, since oil sand is neither tar nor sand. Tar is a residual product that remains after severe thermal cracking of heavy oil, rather than a raw material. Similarly, asphalt and pitch should not be confused with bitumen, because they are actually the residual products after processing of heavy oil or bitumen.

Heavy oil deposits are found in many places in the world with large varieties of types and sizes. Among them, the most explored and biggest reserves are Alberta in Canada, Alaska in the USA, and Orinoco belt in Venezuela. The deposits in Alberta contain very highly viscous hydrocarbons that make it fall into the category of bitumen. In comparison, deposits in Alaska and the Orinoco belt, by definition, belongs to the category of extra heavy oil. (Dusseault, 2001)

## 1.2 SAGD

SAGD is the abbreviation of Steam-Assisted Gravity Drainage, a thermal in-situ heavy oil recovery process.

The SAGD method was invented in the 1978 by Dr. Roger Butler, former holder of Endowed Chair of Petroleum Engineering at University of Calgary in Canada. By 1997, the Underground Test Facility (UTF) project successfully demonstrated that SAGD technology is commercially viable in the Athabasca Oil Sands.

There are several steps in a SAGD process. First, two parallel and horizontal wells are drilled into the oil reservoir, one a few meters above the other, as shown in **Figure 1**. Then, steam is injected into an injection well forming a cone-shaped steam chamber. As the steam chamber expands with time, new heavy oil or bitumen is heated and replaced by steam; the heated bitumen lowers in viscosity and flows downward along the steam chamber boundary into the production well. Finally, the mobile heavy oil is pumped to the surface through the lower production well. This method can improve heavy oil recovery by between 50% and 60% of the original oil in place (OOIP) and is therefore more efficient than most other thermal recovery methods. (Speight, 2013)

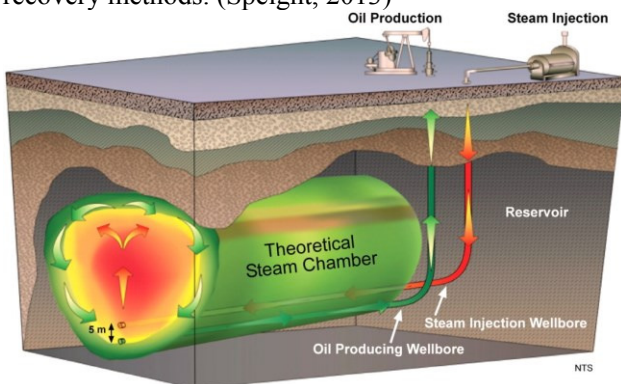


**Figure 1.** Sketch of SAGD process (Purkayastha)

The key benefits of the SAGD process are lower residual oil saturation (SOR), and high ultimate recovery. The issues of this technique relates to low initial oil rate, artificial lifting of heavy oil to the surface, horizontal well operation, and extrapolation of the process to reservoirs with low permeability, low pressure, or bottom water.

### 1.3 AICV

AICV is the abbreviation of Autonomous Inflow Control Valve. It is a technology that can shut off the gas and water autonomously and locally in the production well. It combines the advantages of passive inflow control device (ICD), Autonomous ICD (AICD) and inflow control valves (ICV) used in smart wells.

For most oil production fields, the draining mechanism is based on pressure support from gas and/or water, meaning that gas or water breakthrough will occur after a period of production. Production of oil has to be limited once a breakthrough expands along the horizontal well. Then, the production from the well has to be choked or stopped, although there is still oil left

along the wellbore. ICD and AICD have significantly increased oil production and recovery, however, neither of them is able to completely shut off unwanted gas and water production. The novel AICV technology is a major step for improving oil recovery.

The internal structure of an AICV is shown in **Figure 2**. When oil arrives to the inlet of an AICV, the valve is open and oil can flow from the annulus into the production flow path, as shown in **Figure 3**. In comparison, when less viscous as water and/or gas is reaching the AICV, it keeps closed, which can be seen in **Figure 4**.

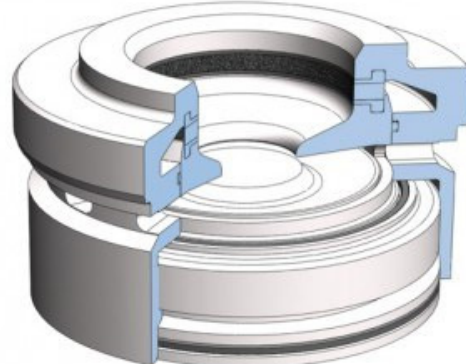


**Figure 2.** Internal structure of an AICV (InflowControl)

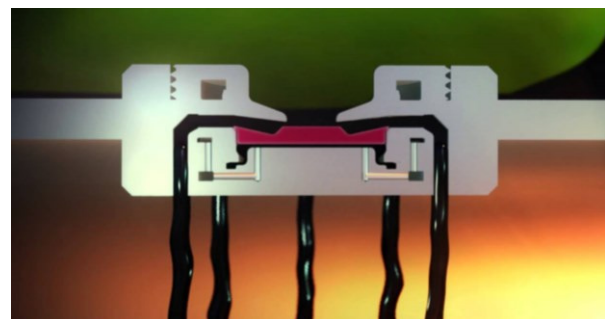


**Figure 3.** Cross-sectional view of AICV at open state (InflowControl)

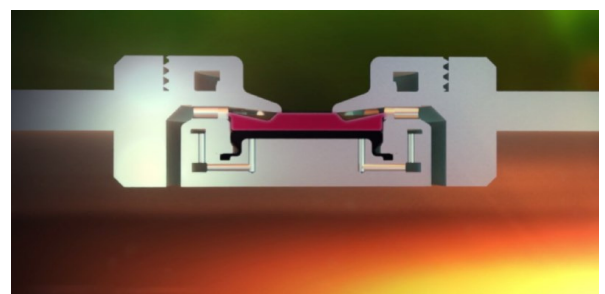


**Figure 4.** Cross-sectional view of AICV at closed state (InflowControl)

For high capacity wells, there is usually laminar flow (viscosity dependent) at the toe. As the cumulative flow increases towards the heel, as a result of friction at the wall of a long well, the flow becomes turbulent (density dependent). The flow rate versus pressure drop is highly non-linear and varies with the degree of depletion.

Pressure drop across the inflow control device is also an important parameter. The restriction has normally turbulent flow which is density dependent and non-linear. The equivalent laminar and turbulent flow restrictors in series can be seen in **Figure 5**.

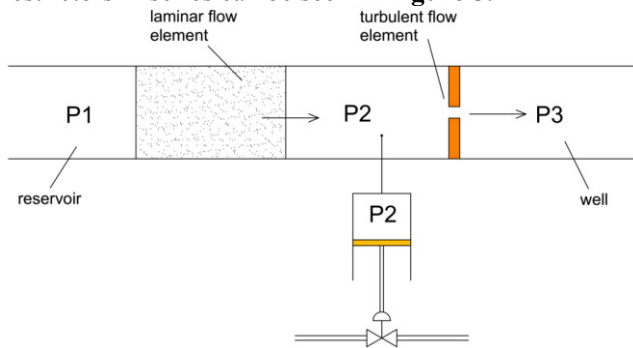


**Figure 5.** Laminar and Turbulent flow restrictors in series

Pressure drop across the laminar and turbulent flow restrictors can be calculated with formula (2) and (3). For turbulent flow restrictor

$$\Delta p = p_2 - p_1 = C \cdot \frac{1}{2} \rho v^2 \propto \rho v^2 \quad (2)$$

For laminar flow restrictor

$$\Delta p = p_2 - p_1 = \frac{32 \mu v L}{D^2} \propto \mu v \quad (3)$$

Based on these equations, the pressure profile along the laminar and turbulent flow restrictors is briefly plotted in **Figure 6**.

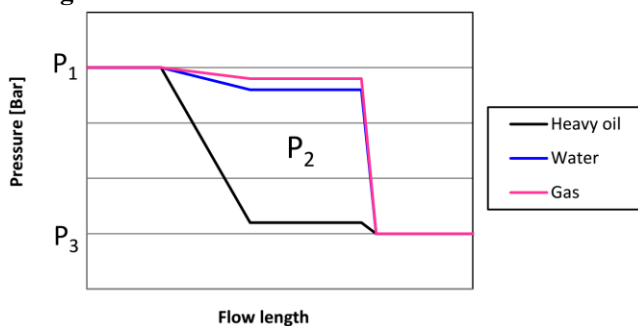


**Figure 6.** Pressure drop along flow length for three phases

Pressure difference between top and bottom sides of AICV is thus caused, depending on the viscosity of fluid flowing through the AICV. By designing different cross-sectional area of top and bottom surface, AICV can be tuned for their automatic opening and closing properties.

AICV can solve gas and water breakthrough problems during heavy oil production. In the SAGD process, steam breakthrough problem can also be avoided by AICV. In summary, AICV can stop unwanted fluid to the well completely; huge potential in oil recovery can be achieved with AICV; AICV gives a more uniform oil production along the well.

## 1.4 Simulation software

In the simulation study, OLGA, ROCX, MATLAB and Tecplot are used.

OLGA is the industry standard tool for transient simulation of multiphase petroleum production. It can be used for well networks, flow lines, pipelines, process equipment, covering the production system from bottom hole to the production system.

ROCX is a near-wellbore reservoir model that can be easily coupled to the OLGA simulator to perform integrated wellbore-reservoir transient simulations. ROCX is a three-dimensional model, capable of simulating three-phase flow in porous media. The OLGA-ROCX coupling is easy to build, robust and numerically stable. (Schlumberger)

MATLAB is used for generation of permeability data string in ROCX. (mathworks, 2015) Tecplot is used for viewing oil and water saturation profiles. (Tecplot)

## 2 Simulation settings

There are two main simulation cases, one with homogeneous reservoir and the other with heterogeneous reservoir. Simulation setting is mainly manipulated through Graphical User Interface (GUI) of OLGA, including flow diagrams, parameters and algorithm.

Before discussing other further content of this paper, it should be stated that one thermodynamic assumption is made. The SAGD process is already at thermal equilibrium once it is initialized, since transient state is not that important for most cases.

### 2.1 General Parameters

The general parameters are used in both homogeneous and heterogeneous reservoir simulations. The meaning of homogeneous reservoir is that the permeability of reservoir does not vary in space, although permeability values of x-y plane is different from that of z direction. For heterogeneous reservoir, permeability varies along x direction. In our case specifically, permeability is lower at all three directions on the left side of the packer (toe) than the right side of the packer (heel).

#### 2.1.1 Reservoir gridding

Because the variations in the y-z plane are of more importance than in the x-direction, the y-z plane is divided into  $31 \times 20$  grids. And since the depth of the reservoir is fixed as 20 m, all dz values are set as 1 m. In comparison, dy values varies with their distance to the production well: the closer the well, the smaller control volumes. This is because the relative importance of accuracy decreases with distance from the well. The dy grid length values are 1, 1, 1, 1.5, 1.5, 1.5, 2, 2, 2, 2.5, 2.5, 2.5, 2.5, 3, 3, with symmetry on the two sides of the well.

In the x direction, the number of grids depends on the number of applied AICVs. In this first case with homogeneous reservoir, there are 3 AICVs and thus  $dx=3$  was set for that case. Notwithstanding, in the case with heterogeneous reservoir with 6 AICVs,  $dx$  was set as 6 accordingly.

### 2.1.2 Other reservoir settings

Porosity is defined as constant 0.3, without variation in space. In order to simplify the problem and reduce calculation time, compression of rock is neglected, and the rock thermal properties are turned off.

Permeability is an important parameter in this simulation study. For heterogeneous reservoir, there are 1860 grid cells, and the string of permeability values is generated in MATLAB and copied into ROCX.

The residual saturation for water, oil and gas are all assumed to be 0. This is because we are more interested in the performance of AICVs, and the simulation time is less than 200 days so the oil is not depleted.

Relative permeability of water and oil  $k_{rw}$  and  $k_{ro}$  are set as manual with the default values in ROCX.

Initial condition of reservoir is the same as the SAGD equilibrium state. Based on this, the boundary conditions for the reservoir are set as 120 °C and 125 bar.

### 2.1.3 Pipeline geometry and thermal properties

The production well consists of the outer annulus and the inner real flow path. The diameter of the annulus is 0.15 m, and 0.12 m for the pipeline. Absolute roughness of the pipeline is  $5 \times 10^{-5}$  m, as material is assumed as slightly corroded carbon steel. Each production zone, corresponding to one AICV, has a length of 20 m.

The mean heat transfer coefficient to the outer wall surface is 6.5 W/(m<sup>2</sup>K). Ambient temperature in the SAGD chamber is set as 120 °C, which is also the initial temperature of the wellbore and the reservoir liquids.

### 2.1.4 Feed liquid properties

Gas specific gravity is 0.64, i.e. 0.64 times of the density of air at 1 atm and 20 °C. Oil specific gravity is 0.85, i.e. 0.85 g/cm<sup>3</sup> as calculated. Viscosity of oil is set as 100 cP, measured at 120 °C and 125 bar, assuming that the production is already in thermal equilibrium. The pressure and temperature value for this measurement is also used as boundary conditions of the production well and the reservoir.

### 2.1.5 Settings for simulated AICV

The diameter of simulated AICV is set as 0.01 m, which is close to the real diameter of a physical AICV. The discharge coefficient is 0.84, which is within the normal range of most valves. The model for the valve

is selected as HYDROVALVE, an OLGA choke model for determining pressure drop and flow rate over the choking range. Stroke time is 0, meaning negligible time for movement, and recovery tuning is 1 giving maximum recovery. The orifice geometry is assumed for the valve, so that there is no spatial extension and vena contracta appearing behind the valve. Moreover, it is also assumed that no slip occurs between gas and liquid.

Besides, the PID controller for the simulated AICV has maximum output signal 1 and minimum output signal 0.008, meaning that the valve can be completely open but not one hundred percent closed. Sample time is 60 s, with bias 0.1 and amplification -0.01; integral constant is set as 50 s.

### 2.1.6 Summary of general parameter settings

The general parameters for the simulation cases are summarized in **Table 1**.

**Table 1.** Fixed parameter settings for simulation

Section	Parameter	Unit	Value
Pipe	Diameter of annulus	m	0.15
	Diameter of inner flow path	m	0.12 m
	Roughness of pipe wall (both annulus and path)	m	$5 \times 10^{-5}$
	Heat transfer coefficient from pipe wall to ambient	W/(m <sup>2</sup> K)	6.5
	Section length for each production zone	m	20
Reservoir	Gridding of reservoir (nx × ny × nz)	[ - ]	$3 \times 31 \times 20$
	Initial oil saturation	[ - ]	1
	Thermodynamic equilibrium temperature	°C	120
	Thermodynamic equilibrium pressure	bar	125
	Specific gravity of gas	[ - ]	0.64
	Specific gravity of oil	[ - ]	0.85
	Porosity of reservoir	[ - ]	0.3
	Viscosity of oil (120 °C and 125 bar)	cP	100
	Diameter of AICV	m	0.01
AICV	Discharge coefficient	[ - ]	0.84
	minimum output	[ - ]	0.008
	Recovery tuning	[ - ]	1
	Stroke time	s	0
	PID controller integral constant	s	50
	PID controller bias	[ - ]	0.1
	PID controller amplification	[ - ]	-0.01
	Controller sample time	s	60
	Controller delay	s	0
	Pressure	Bar	100
Outlet	Temperature	°C	120
Leak	Diameter	m	0.12
	Discharge coefficient	[ - ]	0.84

## 2.2 Model and algorithm

### 2.2.1 Blackoil model

Blackoil modelling allows the user to make a compositional model with minimum input. Details about the fluid composition are not needed for a Blackoil simulation, and the only necessary data is specific gravity of gas and oil and the gas-oil ratio (GOR) at standard conditions. Compared to Compositional Tracking, the Blackoil model is faster in CPU cycles, and it treats shut-in cases more accurately than a standard PVT table option.

Water properties are calculated by the standard OLGA routines. The physical properties of gas and oil are calculated from correlations belonging to a specific blackoil model decided by the user. To find the properties at a specific position in a pipe, the correlations use the pressure, temperature specific gravities of gas, oil and water, as well as GOR at that position. If there are multiple feeds, the specific gravities and GOR are the averages taken over the constituting blackoils weighted by volume at standard conditions.

The Blackoil model is often used when limited specification about the production fluids are available, as during planning or design. Later when production is established, the actual values can be used, and possibly with the module's tuning mechanism to improve the match between observations and predictions made by OLGA.

Assumptions for blackoil model:

1. An oil component cannot exist as gas in the gas phase
2. Gas can dissolve in oil
3. Gas cannot dissolve in the water phase, and water cannot exist as steam in the gas phase

### 2.2.2 Second order scheme TVD method

Mass equations can be solved with two different schemes in OLGA: the first order upwind implicit scheme and the second order Total Variation Diminishing (TVD) scheme. The first order scheme is more robust and should be preferred in most situations, while the second order scheme has less numerical diffusion and therefore keeps holdup fronts better. (Schlumberger)

In the black-oil approach, one mass conservation equation per component in each of the three phases is solved. Also in this approach one pressure equation and one temperature equation (if requested) is solved. PVT data is in this case computed by the user selected black-oil GOR model. And this is also the calculation method in this simulation study.

TVD is short for total variation diminishing, and it is a property of discretization scheme used for solving hyperbolic partial differential equations. For example, in a hyperbolic PDE advection equation (4)

$$\frac{\partial u}{\partial t} + a \frac{\partial u}{\partial x} = 0 \quad (4)$$

The total variation (TV) is given by equation (5)

$$TV = \int \left| \frac{\partial u}{\partial x} \right| \quad (5)$$

Total variation (TV) for the discrete case is (6)

$$TV = \sum_j |u_{j+1} - u_j| \quad (6)$$

Total variation diminishing (TVD) is satisfied if equation (7) is validated.

$$TV(u^{n+1}) \leq TV(u^n) \quad (7)$$

### 2.2.3 Modeling of AICV

In Schlumberger OLGA, an AICV is represented by a transmitter of water cut (WC), a PID controller, a valve, and a leak, as shown in **Figure 7**.

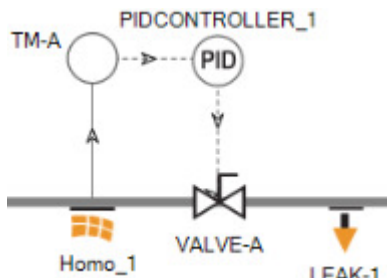


**Figure 7.** AICV model in OLGA graphical user interface

The transmitter (TM-A) measures the value of water cut in the annulus of production well, and send the value to the PID controller (PIDCONTROLLER\_1). The PID controller controls the opening of the valve (VALVE-A), with the controller output calculated by equation (8).

Controller output for a PID controller

$$e(t) = K_p e(t) + K_i \int_0^t e(\tau) d\tau + K_d \frac{d}{dt} e(t) \quad (8)$$

Where:

$K_p$ : Proportional gain

$K_i$ : Integral gain

$K_d$ : Deviation gain

$e$ : Error = SP (setpoint) – PV (process variable)

$t$ : Time or instantaneous time

$\tau$ : variable of integration; takes on values from time 0 to present time  $t$ .

The valve is completely open at the initial time, and only becomes closed when the water cut value in the annulus is higher than the setpoint. The leak (LEAK-1) in **Figure 7** connects the annulus of production well to the inner flow path. Ideally, the pressure drop through the leak is negligible. Relevant parameters of the simulated AICV can be found in section 2.1.5.

## 3 Simulation results

There are two simulation cases demonstrated. One is for homogeneous reservoir with three AICVs and the other is for heterogeneous reservoir with six AICVs.

### 3.1 Simulation of homogeneous reservoir

Main flow diagram of homogeneous reservoir is shown in **Figure 8**.

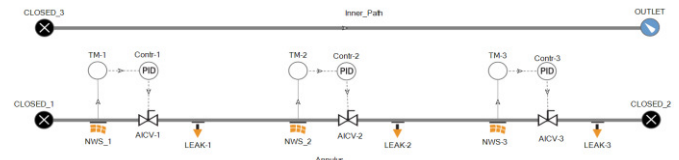


**Figure 8.** Flow diagram of simulation with homogeneous reservoir

There are three near-well sources, each of them connected to one AICV. The reservoir permeability is set as 2000 mD in the x ad y direction and 200 mD at the z direction. Water Cut (WC) is used as set points for the controllers, and is defined as 0.3, 0.6 and 0.9 from left to the right respectively. The relevant results after 120 days of production are simulated and plotted.

#### 3.1.1 Flow rate of oil and water in homogeneous reservoir simulation

Volumetric flow rates of oil and water at the outlet of the production well are plotted as a function of time and presented in **Figure 9**. It should be noticed that the valves cannot be completely closed, since the minimum opening of valves is set to be 0.008 as referred in section 2.1.6.

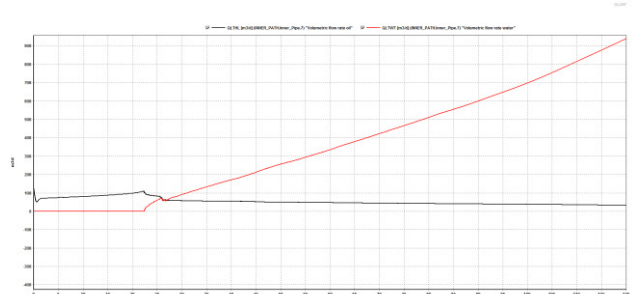


**Figure 9.** Volumetric flow rate of oil and water in homogeneous reservoir simulation

It can be observed that the water breakthrough takes place after 22 days of production, superseding the oil production rate at day 27, whereas the water production continues to increase rapidly with time. At the end time of the simulation, day 120, the water flow rate is 950 m³/d. In comparison, the oil production rate only slightly increases before day 22, and afterwards decreases slowly and continuously. The highest flow rate of oil is 100 m³/d at day 22; at the end time of simulation, this value is only 30 m³/d.

### 3.1.2 Controller signal of AICV in homogeneous reservoir simulation

Trend data of controller signals are plotted in **Figure 10**. Controller 1 (black line) starts to close at day 24 and is completely closed after day 26 days, controller 2 (blue line) starts to close after 30 days and becomes totally closed at day 35 and controller 3 (red line) closes at day 76 and at day 98 it is closed completely.

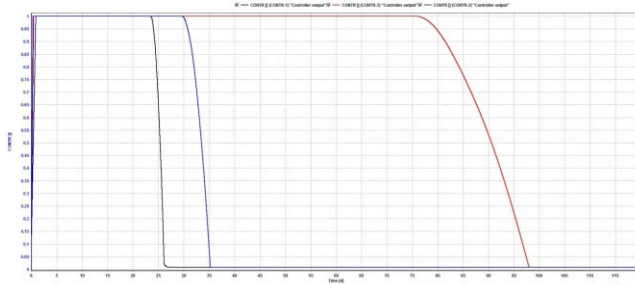


**Figure 10.** Controller output signal for homogeneous reservoir simulation

In order to make it easier to compare the descriptions of controller signal of the homogeneous reservoir, the results are summarized in **Table 2**.

**Table 2.** Controller signal of homogeneous reservoir simulation

Number of AICV	Color	Setpoint	Closing start day (d)	Fully close day (d)
1	black	0.3	24	26
2	blue	0.6	30	35
3	red	0.9	76	98

### 3.1.3 Oil saturation profile of homogeneous reservoir

Oil saturation profiles show the relative distribution of oil and water in the space of reservoirs at a specific time. Variation of oil saturation in y-z plane is of greater interest than along x direction.

The simulation results of oil saturation profiles can be viewed in Tecplot, a software package used in post-processing simulation results. (Tecplot) The oil saturation profiles after 15 days, 30 days, 60 days and 120 days of production are presented from **Figure 11** to **Figure 14**.

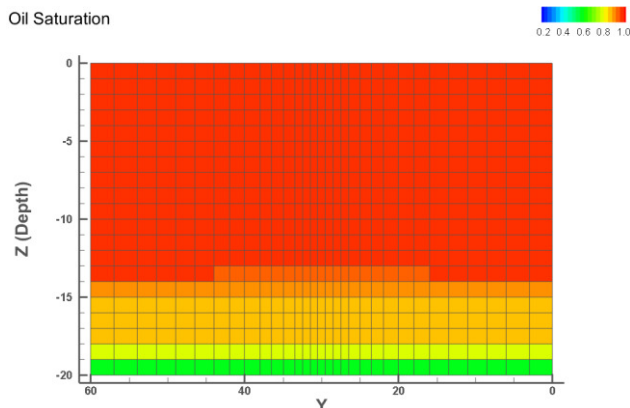


**Figure 11.** Oil saturation after 15 days of production in homogeneous reservoir

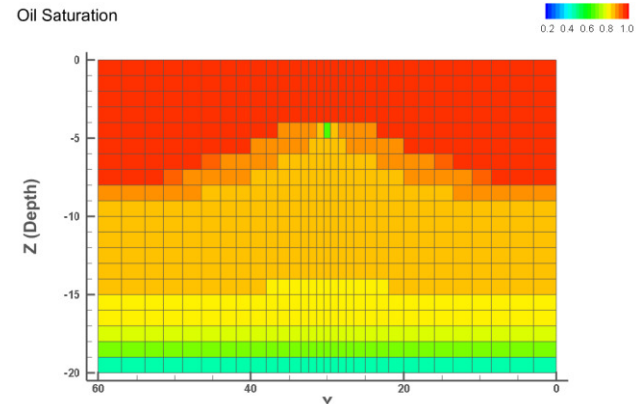


**Figure 12.** Oil saturation after 30 days of production in homogeneous reservoir

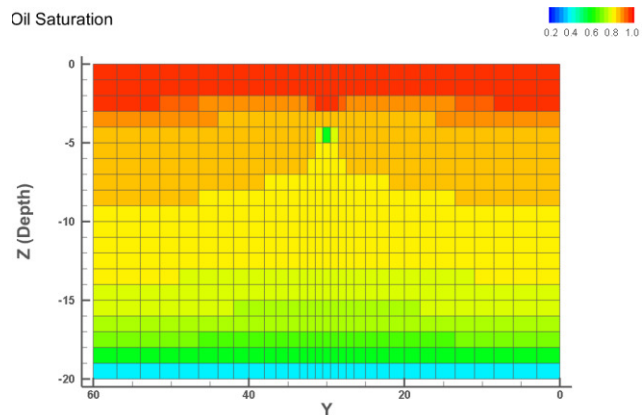


**Figure 13.** Oil saturation after 60 days of production in homogeneous reservoir

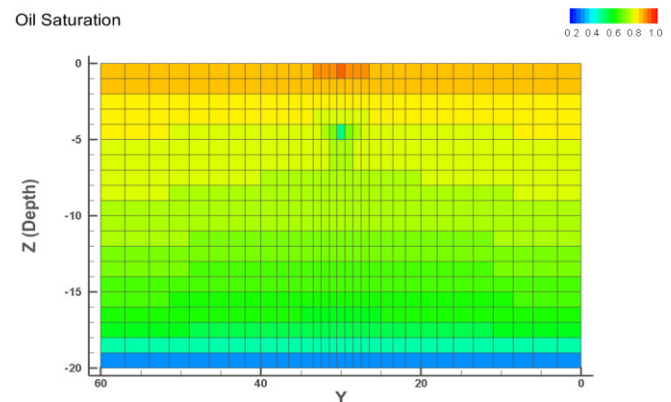


**Figure 14.** Oil saturation after 120 days of production in homogeneous reservoir

It can be seen the oil saturation in the reservoir decreases from the bottom and moves up to the production well with a cone shape (Figure 8 and 9). After the breakthrough of water to the well, the profile of oil saturation continues to increase and has two peaks at each side of the well (Figure 10 and 11).

### 3.2 Simulation of heterogeneous reservoir

The flow diagram of heterogeneous reservoir simulation is shown in **Figure 15**. In this case, there are two production regions, and 3 near-well sources in each region. The two regions are separated by a packer, included as a closed valve in the simulation setting. On the left side of the packer, the reservoir permeability is 2000 mD on x-y plane and 200 mD in z direction. In comparison, on the right side of the packer, the permeability is 5000 mD on x-y plane and 500 mD at z direction.

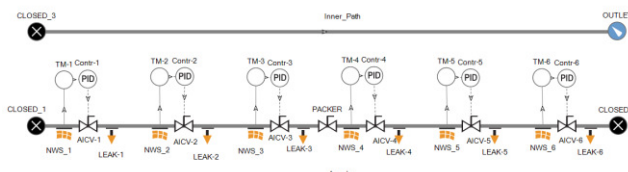


**Figure 15.** Flow diagram of Heterogeneous reservoir simulation

#### 3.2.1 Volumetric flow rate of oil and water

The volumetric flow rates of oil and water production are plotted as presented in **Figure 16**.

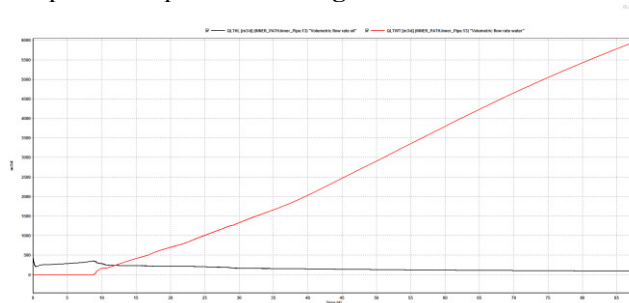


**Figure 16.** Volumetric flow rate of oil and water in homogeneous reservoir simulation

The water flow rate starts to increase rapidly from day 8, becomes higher than oil flow rate at day 12, and continues to increase with time afterwards. At the end day of the simulation, i.e. after 87 days, the volumetric water flow rate is close to  $6000 \text{ m}^3/\text{d}$ .

However, the oil flow rate starts to decrease slowly after water breakthrough from  $390 \text{ m}^3/\text{d}$  at day 8, to  $90 \text{ m}^3/\text{d}$  at day 87.

#### 3.2.2 Controller signal of heterogeneous reservoir

A plot of the six controllers' signal is given in **Figure 17**.

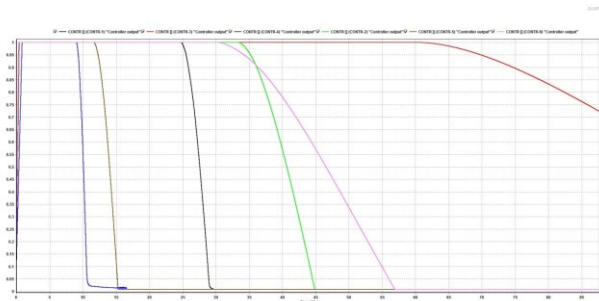


**Figure 17.** Controller output signal for heterogeneous reservoir simulation

The closing order of AICVs is No.4, No.5, No.1, No.6, No.2, and No.3, as shown in the figure. The last one, AICV No.3 is still in the process of closing at the end time of simulation (87 days). The summary of controller signals is listed in **Table 3**.

**Table 3.** Controller signal of heterogeneous reservoir simulation

Number of AICV	Color	Setpoint	Source x-y plane Permeability (mD)	Closing start (d)	Fully close (d)
1	black	0.3	2000	25	29
2	green	0.6	2000	34	45
3	yellow	0.9	2000	61	-
4	blue	0.3	5000	9	11
5	brown	0.6	5000	12	15
6	pink	0.9	5000	30	56

#### 3.2.3 Oil saturation profile of heterogeneous reservoir

For the simulation of the heterogeneous reservoir, the oil saturation variance along the pipeline, x-direction, can be observed from **Figure 18** to **Figure 21**. For example, after 30 days of production, oil saturation at the well position is about 0.75 for both the production regions. However, the neighboring blocks for the low permeable region have clearly higher oil saturation than the high permeable region.

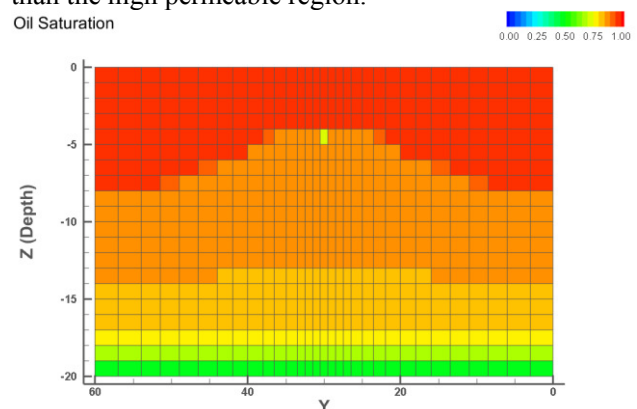


**Figure 18.** Oil saturation profile for I=1 in I-YZ plane after 30 days' production in heterogeneous reservoir

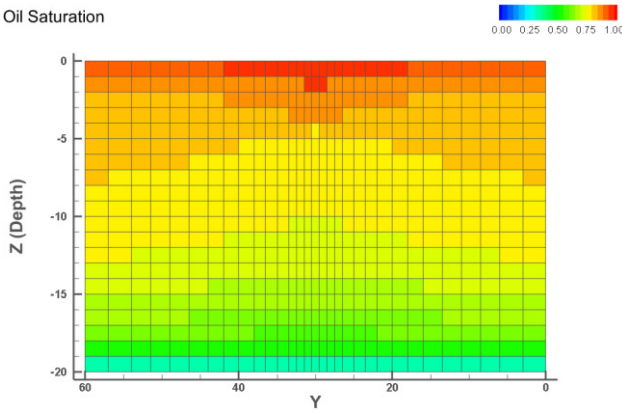


**Figure 19.** Oil saturation profile for I=6 in I-YZ plane after 30 days' production in heterogeneous reservoir

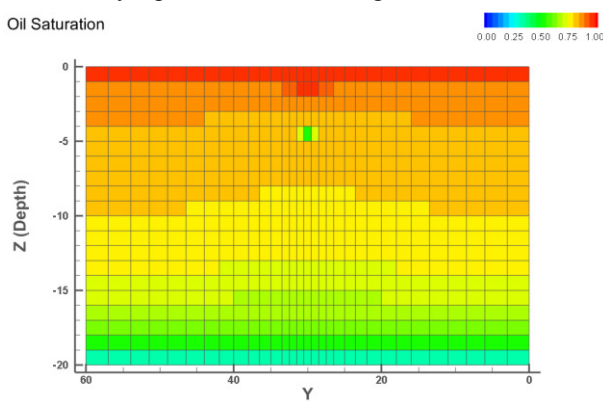


**Figure 20.** Oil saturation profile for I=1 in I-YZ plane after 120 days' production in heterogeneous reservoir

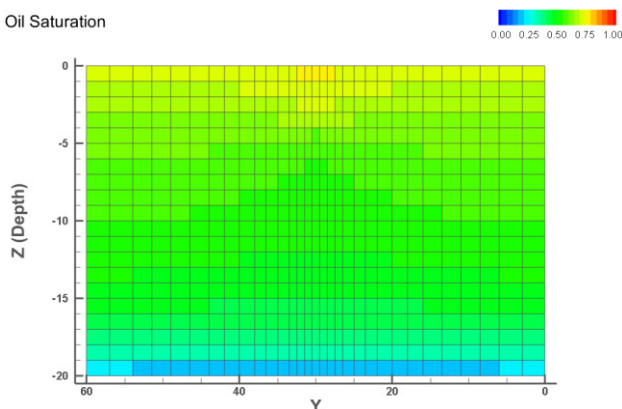


**Figure 21.** Oil saturation profile for I=6 in I-YZ plane after 120 days' production in heterogeneous reservoir

At the end of the simulation, 120 days, the oil saturation is around 0.5 at the location of the production well, as shown in and **Figure 20** and **Figure 21**. The oil saturation values for the neighboring blocks are still at least 0.75 in the low permeable region. But at high permeable regions, oil saturation values for the neighboring blocks are close to 0.5.

## 4 Discussion of results

### 4.1 High production rate of water

In the simulations of both the homogeneous and the heterogeneous reservoir, the volumetric flow rate of water supersedes the oil very soon after water breakthrough, and continues to increase until the end time of the simulation. This phenomenon is due to several reasons. First of all, the viscosity of water is much lower than the viscosity of oil at 125 bar and 120 °C. Secondly, during the production of oil, the oil saturation in the reservoir decreases while the water saturation increases. This causes the relative permeability of oil to decrease and relative permeability of water to increase.

Relative permeability is the ratio of the effective permeability of the actual phase to the absolute permeability. In other words, relative oil permeability is the ratio of effective permeability of oil to the absolute permeability of the reservoir, and similarly for the relative permeability of water.

The formula for calculating relative oil permeability and relative water permeability are given in equations (9) and (10).

Relative oil permeability

$$k_{ro} = \frac{k_{oil}}{k_{reservoir}} \quad (9)$$

Relative water permeability

$$k_{rw} = \frac{k_{water}}{k_{reservoir}} \quad (10)$$

In ROCX, there is a pre-defined series of relative permeability values of oil and water phase, and the plot of those data is shown in **Figure 22**. These values are valid for any arbitrary heavy oil reservoir, but are used in this study.

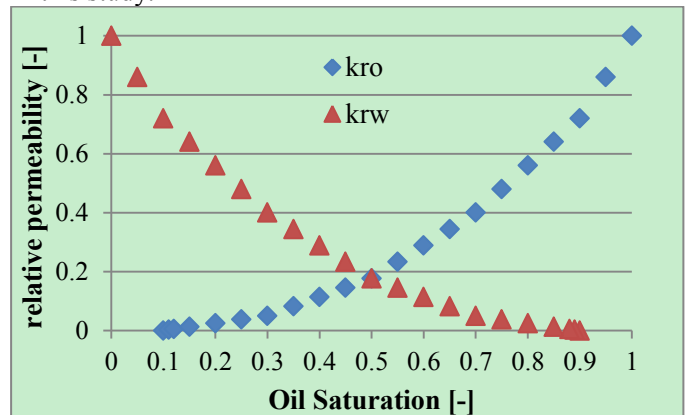


**Figure 22.** Relative permeability of oil and water over different oil saturation

Thus, the relative permeability values for oil and water at any oil saturation can be determined, either by direct reading or linear interpolation. In addition, Darcy's law can be used for calculating volumetric flow rate along a flow path.

Darcy's law for 1-dimensional flow is shown in equation (11).

$$Q = -\frac{kA}{\mu} \cdot \frac{dp}{dx} \quad (11)$$

Where  $Q$  is the discharge rate,  $k$  is the permeability,  $A$  is cross-sectional area of the flow,  $\mu$  is dynamic viscosity, and  $\frac{dp}{dx}$  is pressure gradient along the flow path. All these four parameters influence on the volumetric flow rate of the liquid mixture.

Viscosity of water is a function of temperature and pressure, mainly determined by temperature. Equation (12) shows the temperature dependency of water viscosity (Al-Shemmeri, 2012).

$$\mu(T) = 2.414 \times 10^{\left(\frac{247.8}{T-140}\right)} \quad (12)$$

where  $T$  has unit Kelvin and  $\mu$  has unit  $kg/(m \cdot s)$ . Since the temperature of the SAGD chamber is 120 °C, the calculated dynamic viscosity of water is  $2.30 \times 10^{-4} kg/(m \cdot s)$ , or  $2.30 \times 10^{-7} cP$ . In comparison, the dynamic viscosity of heavy oil is assumed to be 100 cP, much larger than water.

For the near well mixture of oil and water, the only differences between oil and water are the viscosity and the effective permeability, i.e. cross-sectional area and pressure gradient are the same. Thus, the volumetric flow rate of the fluids can be compared by division. Since the relative permeability values of oil and water change with oil saturation, which varies with time, the values of oil saturation must be specified.

Mobility ratio is the ratio between water/oil volumetric flow rates. It depends on viscosity and permeability of water and oil phases.

Equation (13) Mobility ratio

$$\frac{Q_w}{Q_o} = \frac{\mu_o}{\mu_w} \cdot \frac{k_w}{k_o} \quad (13)$$

Mobility ratio can be calculated based on viscosity and relative permeability values of oil and water phase. Mobility ratios with oil saturation 0.2, 0.5 and 0.8 are listed in **Table 4**.

**Table 4.** Mobility ratio with different oil saturation values

Soil [-]	0.2	0.5	0.8
krw [-]	0.56	0.177	0.025
kro [-]	0.025	0.177	0.56
Mobility ratio [-]	9739	435	19.4

It is clear that the ratio between water and oil volumetric flow rate increases rapidly with the depletion of oil. As a result, in the initial period, the oil production rate is relatively high; however, when water breakthrough occurs, the water flow rate increases rapidly. The huge difference between volumetric flow rate of water and oil in the simulation can be understood, given the calculations above.

## 4.2 Controller signal of AICV

It can be observed that the closing performance of valves depends on both permeability of reservoir and set point of controllers, and the later one indicates the strength of the AICVs. Besides, the time it takes for the valves from the start of closing to they are fully closed also depends on those two factors.

The reason for the starting date of AICVs closing is easily understandable. The lower the setpoint, the earlier the setpoint of water cut is reached, since the oil saturation does not change much along the flow path. This can explain well the controller signal for the homogeneous reservoir.

According to the plot of the closing sequence in the heterogeneous reservoir, the other reason that influences the starting date of the closing is the permeability of the reservoir. It is obvious that the higher the permeability, the earlier the closing occurs. Controller 5, although with set point 0.5, even starts closing earlier than controller 1 with set point 0.2, due to the higher permeability.

Another interesting phenomenon is the time it takes for the AICVs to complete the closing progress. The PID controllers for the analogue AICVs have the same parameter settings, except for the setpoint. It can also be observed that the time span for closing the valves increases with increasing setpoint value, as reflected by the homogeneous reservoir simulation. Besides, the time span for the closing also decreases with reservoir permeability, which can be seen from heterogeneous reservoir simulation.

## 4.3 Oil saturation profile

The results of the oil saturation profile are reasonable and matches well with the controller signals.

Initially, only oil is present in the reservoir. As the production goes on, water comes from the bottom of the reservoir. Since the oil specific gravity is set as 0.85, and water at 120 °C and 125 bars has specific gravity 0.949 (peacesoftware: water density calculation), thus water is heavier and comes from the bottom.

In addition, the position of the production well in y-z plane is:  $y=30$  (m) and  $z = -5$  (m). As the production goes on, oil saturation nearest to the well drops firstly, and water continues to fill in the space of removed oil in the reservoir. The more oil produced the lower oil saturation, and the higher water flow rate. Till the time of water breakthrough, a cone-shaped oil saturation profile is formed.

From simulation of the heterogeneous reservoir, the lower permeable (2000 mD) region has larger difference of oil saturation near the production well. At the high permeable (5000 mD) region, neighboring blocks almost have the same oil saturation values as the well. Permeability plays an important role in oil

distribution in the reservoir during the production process.

#### 4.4 Limitations of the study

##### 4.4.1 Insufficient information of reservoir

In this study, a lot of simplifications and assumptions of the parameters of the reservoir are made, due to lack of detailed information for an exact reservoir. These details include geometry, porosity, permeability, relative permeability curves, initial oil and water saturation and fluid phase properties, etc. Among the assumptions and simplifications, there could be one or more that are not reasonable.

##### 4.4.2 Implicit algorithm in OLGA

The mathematical approach in OLGA is implicit and the original program cannot be viewed or modified by users. Although the developers of OLGA programmed the software in a deliberate way, there are still some assumptions and simplifications behind. So, it is also possible that some options of simulation setting are not appropriate, causing imprecise or inaccurate result.

##### 4.4.3 Macroscopic property of OLGA

OLGA is widely-used and powerful software, as discussed before, however, it is more suitable for macroscopic utilities rather than microscopic simulations. In this study specifically, although water cut can be calculated for each section of the pipeline, the exact place where the water is present cannot be approached. To clarify, the interface between water and oil in the annulus is not a perfect plane; oil can be accumulated in one spot for a period of time, meanwhile water is enriched in another spot. This is the case in which AICV shows its proficient ability in shutting down for water and allowing in for oil. Even if the water cut is as high as 0.9, i.e. only 10% is oil in the annulus, oil can still be produced with high purity as long as at least one of the AICVs is covered by oil.

#### 4.5 Prospective improvements

If more details of the reservoir are available, then practical parameters of the reservoir and the fluids can be used. With less assumptions and guesses, the simulation results can be more realistic. The most important parameters include but are not limited to permeability, porosity, relative permeability curve, initial oil and water saturation. All of these parameters can more or less influence the simulation result. Future study could focus on sensitivity analysis for quantifying results uncertainty.

#### 5 Conclusion

In this study, simulations of the SAGD process are performed using the multiphase simulator OLGA in

combination with near well simulation tool ROCX. Since gas breakthrough causes energy loss and lower production rate in SAGD process, AICVs are often used to avoid this problem. In OLGA, a simulated AICV is built up by a normal valve combined with a water-cut transmitter and a PID controller. Controller signals of analogue AICVs have shown that the valves can shut down for water (and thereby also steam), and that the closing time of valves are dependent on WC setpoint of the PID controllers.

Simulations of both homogeneous and heterogeneous reservoirs have shown significant increase of water flow rate after breakthrough. Even when the AICVs are closing one by one and the oil flow rate begins to decrease; the water flow rate continues to increase. This is partly due to much lower viscosity of water compared to oil at high temperature. Another important reason is that water relative permeability increases with oil production. Calculations results show that the volumetric flow rate ratio between water and oil is 19.4 when oil saturation is 0.2, while this ratio changes to 9739 when oil saturation is 0.8.

Tecplot is used to view the results for individual reservoir blocks. The oil saturation profiles in Tecplot well indicate the water breakthrough time in both homogeneous and heterogeneous reservoirs. For the heterogeneous reservoir simulation, oil saturation profiles at regions with different permeability are compared. And it can be seen that the oil saturation has larger differences near the production well in the lower permeable region. This is also reasonable and can be explained by Darcy's law.

There are three main limitations of this simulation study: lack of detailed reservoir information, implicit algorithm, and macroscopic properties in OLGA. The prospect for improvement is to add detailed and practical parameters of a specific reservoir to OLGA and ROCX.

#### References

- Aakre, H. (2015). *Autonomous Inflow Control Valve for Heavy and Extra-Heavy Oil*. SPE International.
- Al-Shemmeri, T. (2012). *Engineering Fluid Mechanics*. Ventus Publishing ApS.
- Alvarez, Johannes, and Sungyun Han. (2013). *Current Overview of Cyclic Steam Injection*. Journal of Petroleum Science Research.
- Banerjee, D. K. (2012). *OIL SANDS, HEAVY OIL & BITUMEN*. Tulsa, Oklahoma: PennWell Corporation.
- Dusseault, M. (2001). *Comparing Venezuelan and Canadian heavy oil and tar sands*. Retrieved from South Portland: [http://www.southportland.org/files/3713/9387/3165/Heavy\\_Oil\\_and\\_Tar\\_Sands.pdf](http://www.southportland.org/files/3713/9387/3165/Heavy_Oil_and_Tar_Sands.pdf)

- Hoffman, B. Todd, and Anthony R. Kovscek. (2003). *Light-Oil Steamdrive in Fractured Low-Permeability Reservoirs*. SPE Western Regional/AAPG Pacific Section Joint Meeting.
- InflowControl. (n.d.). *AICV*. Retrieved from YouTube: <https://www.youtube.com/watch?v=E2g4hxGZP94>
- InflowControl. (n.d.). *AICV Technology*. Retrieved from InflowControl: <http://www.inflowcontrol.no/about-aicv/>
- International Energy Outlook 2010*. (2010). US. Energy Information Administration.
- Jørgensen, Ø. (2010). *Reservoir modelling of lithofacies scale heterogeneities within the middle McMurray formation*. Alberta, Canada.
- mathworks. (2015). *MATLAB*. Retrieved from <http://www.mathworks.com/products/matlab/>
- Meyer, R. F. (2003). *Heavy Oil and Natural Bitumen*. Retrieved from USGS: <http://pubs.usgs.gov/fs/fs070-03/fs070-03.html>
- peacesoftware: water density calculation. (n.d.). Retrieved from peacesoftware: [http://www.peacesoftware.de/einigewerte/calc\\_dampf.php5](http://www.peacesoftware.de/einigewerte/calc_dampf.php5)
- Polikar. (2000). *Fast-SAGD: half the wells and 30% less steam*. SPE/CIM International Conference on Horizontal Well Technology. Society of Petroleum Engineers.
- Purkayastha, S. N. (n.d.). *Control and optimization of steam injection for Steam-Assisted Gravity Drainage (SAGD)*. Retrieved from <http://people.ucalgary.ca/~spurkaya/research.htm>
- Schlumberger. (n.d.). *OLGA Dynamic Multiphase Flow Simulator: User Manual*. Schlumberger.
- Schlumberger. (n.d.). *OLGA ROCX*. Retrieved from [http://www.software.slb.com/store/\\_layouts/SLB/Pages/ProductDetailPage.aspx?pid=AROX-M1](http://www.software.slb.com/store/_layouts/SLB/Pages/ProductDetailPage.aspx?pid=AROX-M1)
- Schlumberger. (n.d.). *Schlumberger OLGA*. Retrieved from <http://www.software.slb.com/products/foundation/Pages/olga.aspx>
- Sheng, J. J. (2011). *Modern Chemical Enhanced Oil Recovery*. Burlington, USA: Gulf Professional Publishing.
- Speight, J. G. (2013). *Heavy oil production processes*. Waltham: Gulf Professional Publishing.
- Tecplot. (n.d.). *Tecplot*. Retrieved from <http://www.tecplot.com/>
- Torsæter, O. (2011). *Heavy oil reservoirs*. Retrieved from NASJONAL FORSKERSKOLE I PETROLEUMSFAG: <http://nfipweb.org/oneday2011/HeavyOilIntroNov11.pdf>
- Yves, A. (2011). *Heavy crude oils: an overview from geology to upgrading*. Ginoux, France: TECHNIP.